

A HYBRID CAPSA-GR-RNN BASED ANALYSIS OF HIGH RENEWABLE ENERGY PENETRATION UNDER THE ELECTRICITY ACT, 2003 FOR SMART GRID SYSTEMS

MANIRAJ PERUMAL¹, Dr. KARTHIKEYAN RAMASAMY², Dr.DURGADEVI VELUSAMY³

¹Assistant Professor, Department of Electrical and Electronics Engineering, M.Kumarasamy College of Engineering, Karur – 639113, Tamilnadu, India.

²Professor, Department of Electrical and Electronics Engineering, M.Kumarasamy College of Engineering, Karur – 639113, Tamilnadu, India.

³Assistant Professor, Department of Information Technology, Sri Sivasubramaniya Nadar College of Engineering, Kalavakkam, Chennai – 603110, Tamilnadu, India.

Corresponding Author: MANIRAJ PERUMAL maniraj.angu@gmail.com¹

Abstract

A Smart Grid System is an advanced electrical grid employing digital communication to enhance electricity flow control, boosting efficiency, reliability, and sustainability of energy distribution. Renewable energy sources, like sunlight, wind, water, and biomass, offer clean and sustainable energy but suffer from intermittency due to weather variations and can lead to land use conflicts as hefty installations may compete with agriculture or natural environments. The Capuchin Search Algorithm (CapSA) and Global-Context Residual Recurrent Neural Networks (GR-RNN) work together to create the CapSA-GR-RNN Approach, a hybrid method for smart grid systems with high penetration of renewable energy sources (RES). The main goal of the proposed technique is to reduce operational cost, pollution emission, and maximize availability by using RES. CapSA is used to optimize the performance of smart microgrids, and GR-RNN is used to predict the behavior of RES, such as the Probability Density Function (PDF) and Cumulative Density Function (CDF). This method has been implemented on the MATLAB platform. The proposed method is compared with existing methods such as Particle Swarm Optimization (PSO), Grey Wolf Optimizer and Sparrow Search Algorithm,. In the proposed approach, the cost is \$0.93, whereas the existing methods incur costs of \$1.08, \$0.96, and \$0.98. This indicates that the proposed method has a potential cost saving capability linked to the existing methods.

Keywords: Direct Current, Energy Storage System, Fuel Cell, Load, Photo Voltaic, Smart Grid, Wind Turbine.

Introduction

a. Background

Recent research on energy optimization suggests that it's possible to reduce energy consumption by 25-35% without altering existing system infrastructure through the optimization of power usage and generation [1]. One way to lower pollution emissions, satisfy customer demands affordably, and reduce power loss is to employ RES like solar and wind [2]. Energy optimisation has become a significant problem with the emergence of the notion of a highly integrated renewable energy source-based Smart Grid (SG) [3]. Power companies may combine various renewable energy sources and make better selections when it comes to wind and solar energy systems to increase the power system overall reliability of the become more integrated into current power systems and show greater flexibility in smart grid operations [4-5]. Moreover, with the daily rise in electrical energy demand, there's a pressing need for reliable energy sources to meet future energy requirements, with solar-wind hybrid energy systems emerging as a promising solution [6-7]. This article's main goal is to increase power systems' reliability by



incorporating solar and wind energy sources into existing networks. utilising cutting-edge, clever tactics [8]. Due to the rapid rise in renewable energy, the integration of solar and wind power increases the complexity of the system, leading to increased failure rates. These failures are often attributed to adverse operating conditions and fluctuating loads [9-10]. In solar photovoltaic systems, the primary components include PV modules and their accessories, while in wind energy systems; the gearbox plays a pivotal role. Gearboxes are essential for transmitting torque and regulating speed in wind turbines [10-11].

b. Literature review

The literature has already reported many studies focusing on smart grid systems with substantial penetration of RES and features. Some of them reviewed are as follows,

M. Fotopoulou et al. [12] have suggested a technique to evaluate how well smart grids perform in emergency scenarios. Smart grids, with all its fancy optimisation algorithms, don't always function without emergencies requiring changes to the EMS via a DSS. The aim of this study is to assess how crises affect smart grids by employing a unique optimisation method. The approach incorporates Artificial Neural Networks (ANN) for intermittent RES production forecasting and an optimizer to improve the grid's autonomy by prioritising RES. Each emergency scenario was evaluated based on its effect on grid autonomy, sustainability, curtailments, and CO2 emissions. I. Akhtar et al. [13] have suggested a reliability analysis of power systems that takes into account the advanced intelligent techniques for RES integration. As the power industry transitions towards more secure and advanced smart grids, incorporating RES like solar and wind energy systems becomes crucial for achieving reliability and security goals. This article's objective is to improve the dependability of the power system by skillfully integrating solar and wind energy into the system. It covers several models and frameworks that may be used to evaluate the reliability effect of RES integration. K. Liang et al. [14] have suggested rehabilitation of the electricity system in the context of widespread use of renewable energy, the difficulties in restoring power systems that come with integrating a lot of renewable energy. It outlines stages of transmission and distribution system restoration processes, highlighting advances in handling renewable power uncertainty during restoration. The paper discusses various techniques, including microgrids, multi-agent systems, and flexible resource utilization, to ensure efficient restoration with large renewable energy penetration.

S. Saha *et al.* [15] have suggested the impact of growing grid frequency behaviour on renewable energy source uptake. The grid's inertia reduces as inverter-based RES take the place of conventional synchronous generators, which presents problems for the frequency stability of the grid. Integrating inverter-based renewable energy sources into the grid frequency responsiveness is assessed in this study through the use of eigenvalue analysis of low-inertia power networks. S. Wang *et al.* [16] have suggested the requirement for energy storage for frequency control and peak shaving in power networks with high renewable energy penetration. The recommended method for estimating the energy storage capacity needed in such systems to optimise system operating costs while accounting for net load uncertainties and peak shaving and frequency control. L. Wang et al., in [17], suggested a unique energy management method with blockchain technology for dispersed energy networks with large diffusion of renewable energy. The paper streamlines the model inversion procedure for blockchain encryption methods and provides a consensus mechanism based on proof of energy contribution. This dynamic energy management mode is designed to solve the problems of distributed and independent energy management in systems with a high penetration of green energy. In order to expand the use of dispersed



renewable energy in smart grids, J. Hashimoto et al. [18] proposed an advanced technique for grid integration. With the increasing use of generators powered by renewable energy, there was a need for robust testing platforms to assess their impact on grid operations. The paper proposes an advanced testing platform to ensure compliance with grid integration requirements and streamline testing processes for connected devices in smart grids.

c. Research Gap and Motivation

The most difficult issues are those related to developing a smart grid system with a tall RES penetration, according to a general overview of recent studies. Drawbacks include the complexity of the hybrid method and potential challenges in real-world implementation due to the intricate combination of optimization techniques. An ideal method introduces an optimal power flow for HRES that makes use of the Sparrow Search Algorithm (SSA) and Improved Bear Smell Search (IBSS). Therefore, in order to maintain an excellent inverter output, adequate fluctuation balancing and the acquisition of an advanced controller are required. Fuzzy logic control and model predictive control systems can be used in an advanced control system to overcome this issue. Another significant challenge is ensuring grid resilience and stability when there is a high RES penetration rate. The intermittent nature of renewable energy generation can result in sudden fluctuations in power supply, potentially foremost to voltage then frequency instability. Optimal approaches for HRES power quality enhancement are needed to overcome these obstacles. However, since of the erratic and recurrent nature of RES energy optimisation and consumer behaviour, is difficult. Previous research has attempted to address this challenge using various optimization techniques, such as hybrid optimization schemes (GSA-PSO), optimization-centric strategies (DP, PMP, ECMS, and PSO), ANN, and state-of-the-art energy dispatch algorithms. Optimal strategies for great penetration of HRES are needed to overcome these obstacles. These drawbacks are motivated to do this work.

d. Challenges

One of the primary challenges in optimizing energy from RES similar to sun and wind, their behaviour is unpredictable, leading to discrepancies between real-time generation and forecasted values. This uncertainty poses difficulties for smart grid (SG) operators tasked with balancing energy generation and consumption. To mitigate this, operators maintain reserves to address fluctuations in energy generation and uphold security levels. However, existing models, while suitable for such scenarios, face performance degradation when scaled. Additionally, approaches such as the scenario tree method are employed to tackle energy management issues. However, because of the erratic and irregular nature of RES and customer behaviour, the optimisation process is still difficult.

e. Contribution

The following a summary of this manuscript's primary contributions:

- This manuscript presents a novel hybrid method for enhancing the efficiency of smart grid systems with a high penetration of RES.
- The proposed hybrid technique integrates the CapSA with GR-RNN. The main objective of this proposed method is to minimize operational costs, decrease pollution emissions, and maximize resource availability through RES utilization.
- In this hybrid technique, the GR-RNN models PDF and CDF to forecast the behaviour of RES, namely solar and wind, while the CapSA method is used to maximise the performance of smart microgrids.



• The performance of the proposed strategy is assessed by implementing it in MATLAB and comparing it to other approaches.

f. Organization

The remaining part of the research article is as: Sector 2 depicts the Summary of the hybrid energy system with PV, wind turbine, and battery. Proposed method for smart grid system with renewable energy sources using hybrid CapSA-GR-RNN approach is represented in sector 3. Sector 4 represents the results and argument while Sector 5 gives the conclusion of the manuscript.

2. Conformation of the Hybrid Energy System with Battery, Wind Turbine and PV

Configuration of the hybrid energy system with battery, wind turbine and PV is shown in Fig 1. The smooth incorporation of RES like PV and wind power into a smart grid system involves a dynamic interplay among these decentralized energy generation systems, the traditional utility grid, and potential additional distributed energy resources such as fuel cells. PV systems harness sunlight to generate electricity through photovoltaic panels, while wind turbines fed power to the grid by utilizing the kinetic energy from the wind. Both PV and wind systems generally feed the generated electricity into the local distribution grid. Smart grid technologies enable bidirectional communication between these distributed energy resources and the utility grid, control of energy flows and allowing for real-time monitoring. This capability empowers grid operators to effectively manage the intermittent nature of renewable energy sources, thereby optimizing their integration while upholding reliability and stability. Concurrently, fuel cells present another avenue for distributed energy generation that can be seamlessly integrated into the smart grid ecosystem. Operating through electrochemical reactions, fuel cells often utilize hydrogen or natural gas as fuel to produce electricity. They complement renewable energy sources by offering continuous or dispatch able power generation capabilities. Smart grid integration enables the coordinated operation of fuel cells alongside other renewable sources, optimizing their utilization based on variables including grid limitations, renewable energy supply, and energy consumption. The CapSA-GR-RNN approach combines CapSA and GR-RNN to enhance smart microgrid efficiency, emphasizing RES forecasting. It also incorporates a DC/DC converter to optimize energy flow management within the microgrid.



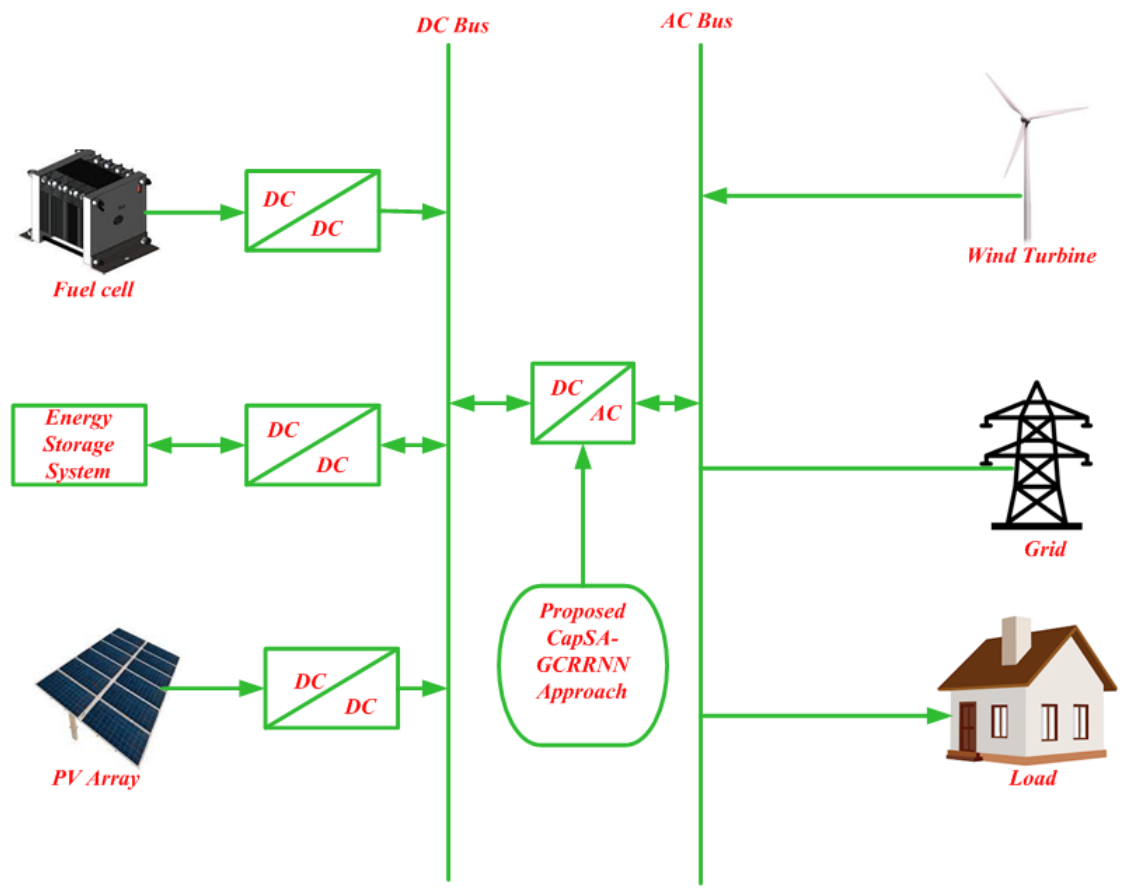


Fig 1: Configuration of the hybrid energy system with battery, wind turbine and PV

2.1. Modeling of PV system

Solar energy is instantly transformed to electrical energy by the PV. PV cell circuit includes diode and current source (I_{ph}) [19]. A p-n junction is inferred using the anti-parallel diode, and solar radiation is emulated by the current source. Shunt and series resistance are incorporated in PV cells to reduce losses, and solar irradiance causes them to produce DC when sunlight touches them. When Kirchhoff's Current Law (KCL) is applied to the circuit above, the output current for PV is achieved as,

$$I_{pv} = I_{ph} - I_D - I_{sh} \tag{1}$$

In this case, I_{ph} for ID for the diode current, photocurrent, I_{pv} stands for the PV current, and I_{sh} for the shunt current. In terms of the diode current,

$$I_D = I_o \left(e^{\frac{V_{pv} + IR_s}{V_T}} - 1 \right)$$
 (2)



Where, I_o is used to represent the saturation current, V_T is denoted as the voltage at room temperature, V_{pv} the PV voltage, and R_s is represented as the series resistance. To express the thermal voltage,

$$V_T = k.T_c/q \tag{3}$$

$$I_{ph} = \frac{G}{G_{ref}} \left(I_{ph,ref} + \mu_{sc} . \Delta T \right) \tag{4}$$

Where, G stands for irradiance $I_{ph,ref}$ attitudes for the photocurrent below standard test conditions, G_{ref} for the irradiance, and $T_{C,ref}$ is the temperature of the cell. $T = T_C - T_{C,ref}$, where sc for the SC current's temperature coefficient. Shunt current is given by,

$$I_{sh} = \frac{V_{pv} + IR_s}{R_{sh}} \tag{5}$$

Where R_{sh} is castoff to denote shunt confrontation. The PV system's concluding equation for current is given as,

$$I_{pv} = I_{ph} - I_o \left(\exp \frac{q(V_{pv} + R_s I)}{N_s kT} - 1 \right) - \frac{V_{pv} + R_s I}{R_{sh}}$$
 (6)

Here, N_s signifies the quantity of cells in series and q stands for the electron charge denoted by q. A solar cell's low DC voltage can be maximized by using a Re-lift Luo converter.

2.2. Equation Modeling of Wind turbines

The gale's velocity and the region it travels across determine how much electricity a wind turbine can generate [20]. A wind turbine's power may be computed as follows:

$$P_{WT}(T) = \begin{cases} 0 & A(T) \le A_{cin} \text{ or } A(T) \ge A_{coff} \\ P_R^W \frac{A(T) - A_{cin}}{A_R - A_{cin}} & A_{cin} < A(T) < A_R \\ P_R^W & A_R \le A(T) < A_{coff} \end{cases}$$

$$(7)$$

Where, A(T) is the vital height of the wind speed, A_{coff} is represented as the cut-off speed, P_R^W is indicated as the rated power of the wind turbine, A_{cin} is indicated as denoted is the rated wind speed, and as the cut-in speed,

The probability density function (PDF) is a curve that illustrates the variation of wind speed throughout the year. The area under the curve could be depicted to represent the probability that the wind will fall between two given wind speeds when the changing wind speeds are considered. It could be specified as:

$$P(a_1 \le a \le a_2) = \int_{a_1}^{a_2} E_a da \tag{8}$$

$$P(0 \le a \le \infty) = \int_0^\infty E_a da = 1 \tag{9}$$

Where, E_a is the wind speed PDF, a_1 and a_2 are the 2 wind speed systems. The Weibull probability function, which forms the basis for characterising wind speed statistics, is defined as:



$$E_a = \frac{k}{c} \left(\frac{a}{c} \right)^{k-1} \exp \left(\left(-\frac{a}{c} \right)^k \right) \tag{10}$$

Here, k is denoted as the shape limit, c is indicated as the scale parameter, and a is represented as the wind speed system. The Weibull probability function is the most important PDF for wind speed statistics

The wind speed of the earth's surfaces varies; for instance, the wind speed over a forest and a calm sea varies. This difference can be computed through determining the wind speed at an increased height. The following is how to calculate the speed of wind at an attained height:

$$A = A_0 \left(\frac{H_{wt}}{H_0}\right)^{\alpha} \tag{11}$$

Where, A is represented as the wind speed at a required height H_{wt} , A_0 is indicated as the wind speed at a reference height H_0 , and α is indicated as the friction coefficient. The friction coefficient is determined by the topography that the wind blows over. In general, it is thought that an approximate value for α is 1/7.

The computation of the total power $P_{wt}(T)$ generated by wind turbines is as follows:

$$P_{wt}(T) = N_{wt} P_{WT}(T) \tag{12}$$

Where, N_{wt} is the quantity of turbines.

2.3. Fuel Cell Model

Using Hydrogen Fuel Cells (HCs), energy is produced through the electrochemical reaction of oxygen and hydrogen [21]. PEM fuel cells are the most widely used type of FCs in automotive applications, notwithstanding their variety. In such instance, the car was outfitted with an *Horizon* H-3000 open cathode PEMFC, this has a maximum output of 3000W and 72 cells. Our special technology replaced the original control system, which lets hydrogen circulate through a Venture ejector. For this study, the fuel cell model is simplified into a quasi-static model that comprises a fuel usage map and some limits. If the temperature inside the stack isn't large enough, the stack voltage drops, and the fuel cell can produce up to 3000 watts., cannot operate at its full power. Under these circumstances, a low voltage failure might manifest, causing the FC to stop working. The FC can run at up to 2100W maximum power. On the other hand, FC power is defined as gross power less the power of auxiliary components, or net power. However, as the FC has a minimum power authorization of 0, it is in standby mode.

The power gradient in the FC is:

$$\Delta P_{FC}(n) = \frac{P_{FC}(n) - P_{FC}(n-1)}{t_s},$$

(13)

As we shall see later, this value represents the control input that the EMS calculates, where $P_{FC}(n)$ is the power given by FC. Control input is thus limited in the following ways:

$$0 \le P_{FC}(n) \le 2100,$$

(14)

$$-900 \le \Delta P_{FC}(n) \le 300.$$

(15)



Notice that Equation (15) depends on the real power values and the preceding ones. To overcome these limitations, using the following state equation as a guide, one method is to study the power in the FC as a state variables as:

$$s_{FC}(n+1) = P_{FC}(n)$$
.

(16)

Now, the constraint in Equation (15) is contingent on a state. Generally speaking, this limitation places severe restrictions on the EMS, which significantly degrades the vehicle's performance. Lastly, the gross current can be used to determine the consumption. One way to calculate the instantaneous fuel usage is as follows:

$$m_{H_2} = i_{FC,gross} \frac{0.03761}{3600} N_{cell} \tag{17}$$

Where, m_{H_2} is denoted as the H_2 mass flow rate in g/s, $i_{FC,gross}$ is indicated as the gross current (i.e. stack current) in amperes, and N_{cell} is denoted as the number of cells of the FC stack. Solitary the H_2 reactions have been taken into account thus far. The H_2 emitted during purges is another, though less significant, role in the consumption. It is challenging to predict or replicate by modelling the quantity of H_2 emitted during purges. Counting solely the H_2 reactions in the stack's cells, the comparison of fuel consumption is done on the assumption that the amount of fuel used is independent of the EMS selected.

2.4. Objective Function

Certain and uncertain costs make up the two primary types of operational costs. Demand Response Programmes (DRPS), power costs purchased from or sold to the utility, and Distributed generation (DGS) startup and operation costs are two instances of specific operating expenses [22]. On the other hand, reserve costs supplied by DGS are also included in this category. Wind and solar parameter uncertainty affects the probability of scenarios (Prs). The Value of Lost Load (VOLL) expenses, DGS unit running costs, load decrease from implementation, and user Expected Energy Not Served (EENS) prices are all examples of uncertain operational costs.

$$M = \min F_1(X) = \sum_{t=1}^t sf^{\cos t(t)} = \sum_{t=1}^t sCOC(t) + \sum_{t=1}^t s\sum_{p=1}^p \Pr_s \times UOC_p(t)$$
(18)

Wherever, Pr_s is the probability of scenarios. The two types of operational costs are known as definite and uncertain, respectively. T is denoted as the time. Here, D denoted as the total operating cost.

The pollution emission function encompasses emissions generated by activities such as DGS operation and emissions resulting from grid purchases. Pollutants considered include CO₂, SO₂, and NO₂. This allows for the derivation of a statistical model for the pollution function.

$$\min F_2(X) = \sum_{t=1}^{emmission(t)} f^{emmission(t)} = \sum_{i=1}^{emmission(t)} [e_{mi_{DG}}(t) + e_{mi_{gird}}(t)]$$
(19)

Here, t is denoted as the time, e is denoted as the actual wind speed of wind turbine.

3. Proposed Methods for Smart Grid System with Renewable Energy Sources



This paper proposes a smart grid system with renewable energy sources using hybrid CapSA GR-RNN approach. The GR-RNN approach is used to forecast the behaviour of RES, such as solar and wind PDF and CDF, while the CapSA is used to maximise the performance of smart microgrids. This proposed method to evaluate the performance of smart grid systems amidst high integration of RES. By combining the optimization capability of CapSA with the predictive power of GR-RNN, the research aims to provide a comprehensive assessment framework for smart grid operations under diverse conditions.

3.1. Capuchin Search Algorithm

The CapSA impersonators the active lifestyle of these primates in the wild, drawing inspiration from their foraging habits. The CapSA is used to optimize the performance of smart microgrids. Just as capuchins balance exploration of new foraging areas with exploitation of known food sources, In order to take advantage of promising answers and explore new areas of the solution space, the algorithm dynamically modifies. It introduces randomness and diversity akin to the capuchins' varied foraging behaviors, while also making effective use of global and local search techniques to traverse complicated solution spaces. Through iterative improvement, the algorithm converges towards optimal or near-optimal solutions, reflecting the adaptive nature and problem-solving prowess observed in capuchin monkey life. Capuchin monkeys move about and roam around on the ground and in trees in search of food sources [23]. CapSA Flowchart is depicted in Fig 2.

Step 1: Initialization

To initialize the input factors such as solar irradiance, current, voltage and wind speed.

Step 2: Random Generation

Following setup, the accidental vectors generate the input limits at random.

$$Y = \begin{bmatrix} Y_{1,1} & Y_{1,2} & \dots & Y_{1,d} \\ Y_{2,1} & Y_{2,1} & \dots & Y_{2,d} \\ \dots & \dots & \dots & \dots \\ Y_{n,1} & Y_{n,1} & \dots & Y_{n,d} \end{bmatrix}$$
(20)

Where, n is indicated as the prime parameter and d is denoted as the dimension of the desirable variables.

Step 3: Fitness Calculation

The goal function is used to pick the fitness and is represented as,

$$F = \min(M) \tag{21}$$

Where, M denoted as the total operating cost.

Step 4: Exploration Phase

Exploration frequently entails introducing randomness into the search process, which may involve generating new candidate solutions through mutation or random sampling. The proposed technique finds global solutions that represent food sources to solve optimisation problems with predetermined dimensions, as was previously described. This is accomplished by repeatedly revising the stances of leaders and followers until they converge on the global solutions, or food sources. As a result, the proposed algorithm's computational complexity is defined as follows:

$$o(V(k(PD+PC)))$$
 (22)



Where, V is denoted as the quantity of testing experiments, K is indicated as the most iterations possible, P is denotes the amount of solutions, D is indicates the maximum quantity of retries feasible, and C denotes the price of the optimisation problem's objective function.

Step 5: Exploitation Phase

Any meta-heuristic algorithm's efficacy is determined on how well it can reconcile the needs of exploration and exploitation. First, the algorithm uses a predetermined number of solutions from the population of capuchins to explore the search space. As the search progresses and the algorithm seek food sources, the emphasis on exploration decreases while exploitation becomes more prominent. Exploitation entails utilizing promising solutions already discovered to further enhance their quality.

Step 6: Update the Best Solution

This experimental test's objective is to evaluate CapSA's exploring capabilities, particularly on fixed-dimension multimodal functions. Additionally, CapSA is noted for its consistently low Standard Deviation (STD) values across various functions compared to other optimization algorithms. All things considered, the average and standard deviation of the best solutions found after thirty separate runs show that CapSA reliably produces higher performance levels. In this context, the lifetime of CapSA is managed through an exponential function proposed within the algorithm to, as Equation (23), illustrate, efficiently strike a balance between exploitation and exploration throughout both local and global search operations.

$$\tau = \beta_0 E^{-\beta_1 \left(\frac{K}{k}\right)^{\beta_2}} \tag{23}$$

Here, K and k denote the current iterations and values of the maximum, correspondingly. The parameters β_0 , β_1 , β_2 remain chosen at random to be 2, 21, and 2. The proposed approach explores the search space with a suitable number of solutions using the exponential function τ , with each search region being used by the individuals in order to identify the best solutions.

Step 7: Termination

The process halts when the solution is deemed the best possible, but if it's not, it goes back to Step 3 where it calculates fitness and continues with the following steps until the best solution is found..



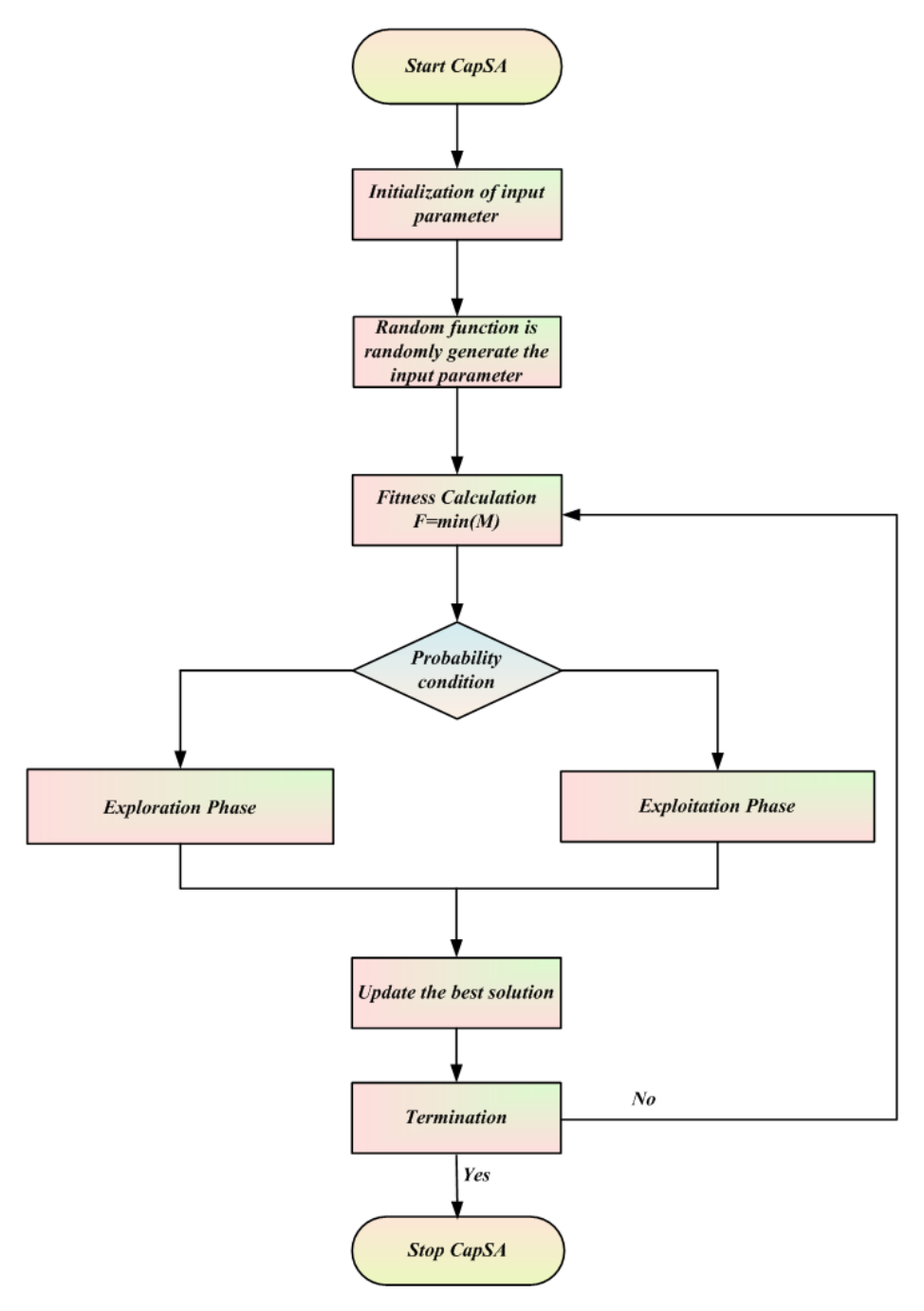


Fig 2: Flow Chart of CapSA

3.2. Global-Context Residual Recurrent Neural Networks (GCR-RNN)



The segmentation sequence of the local feature is combined with the global-context data in the proposed residual RNN block, is explained in detail in this section.

Each sequence fragment's feature vector is acquired by means of global average pooling, yielding a feature vector of size. The feature dimension is then increased from 256 to 512 using a Fully-Connected (FC) layer, which brings it into alignment with the global-context feature. To capture the spatial relationships of each fragment, the feature vector sequence is subsequently input into Gated Recurrent Units (GRU) [24]. The following is the definition of GRU, a simplified recurrent neural network enhanced:

$$z_{t} = \sigma \left(W_{2} x_{t} + U_{z} F^{t-1} + V_{z} \right) \tag{24}$$

$$r_t = \sigma \Big(W_r x_t + U_r F^{t-1} + V_r \Big) \tag{25}$$

$$h_t = \phi \Big(W_h x_t + U_h \Big(r_t \otimes F^{t-1} \Big) + V_h \Big) \tag{26}$$

$$F^{t} = z_{t} \otimes F^{t-1} + (1 - z_{t}) \otimes h_{t} \tag{27}$$

Here, F^t is indicated as the global context feature at the time step t and x_t is denoted as the fragment feature vector z_t and r_t are represented as the sigmoid is used to reset and update the gates $\sigma(x)$ as the activation function. $\phi(x)$ is represented as the tangent function hyperbolic and W_*, U_*, b_* are represented as the training-induced parameters. The GRU is represented by

$$F^{t} = GRU(x_{t}, F^{t-1}) \tag{28}$$

Inspired by the residual network, it proposes the global-context residual GRU as follows to fully using the local fragmentary characteristics' handwriting style information:

$$F^{t} = GRU(x_{t}, F^{t-1}) + x_{t} t \in \{1, 2, \dots, 8\}, F^{0} = F_{G}$$
 (29)

Here the local feature x_t at time step t is used by RNN to update and enhance the feature vector F^t , which is initialised by the global-context F_G . Each feature vector F^t that is produced as a result of GRU's context modelling includes both local and global discriminative information.

$$F = \sum_{t=1}^{8} F^{t} \tag{30}$$

Ultimately, the input image's final feature vector, F, is calculated using:

Continuing from the previous context, we then have a classifier with a soft-max layer comprising N output neurons. Where F refers to the feature vector. Finding a DCRNN model and training a FNN on it for the purpose of choosing an OC policy are the two steps of the RCNN training challenge. First, we describe the RNN (and DCRNN) training issue. Next, we provide the DCRNN model extension as the basis for the RCNN and outline its training issue. Assume that a nonlinear open-loop dynamical system governs the dynamics of the environment or system process, and that the model is unknown. Let $\{U_0, U_1, ..., U_{n-1}\}$ be an order of the dynamical system's inputs and $\{Y_0, Y_1, ..., Y_{n-1}\}$ the matching series of tangible results, with $U_s \in r^{eU}$, $Y_s \in r^{eV}$. To identify a system, one trains an RNN model in the format

$$X_{T+1} = f_X(X_T, Y_T, U_T, \theta_X)$$
(31)

$$\hat{Y} = f_Y(X_T, \theta_X) \tag{32}$$



The Markovian state-space dynamics are explained by f_X and f_Y , which are respectively parameterized by the weight/bias factors of victories and $\theta_X \in r^{e\theta_X}$ and $\theta_Y \in r^{e\theta_Y}$. The RNN hidden state is represented by $X_e \in r^{eX}$, and its forecast for the system visible at time T is represented by $\hat{Y}_e \in r^{eY}$. The purpose of the identification job is to train the RNN to encode relevant information about the hidden states X_T of the genuine system. Apart from being supplied as external inputs to the state-update function, the observables Y_e are also assigned as the targets for the RNN predictions \hat{Y}_e . The idea behind this study is to learn X_e and the parameter vectors θ_X , θ_Y simultaneously in the context, which is similar to the direct multiple firing method to OC issues. In order to do this, the learning goal is formulated as an equality-constrained problem.

$$\min_{Z} F(Z) := r(X_0, \theta_X, \theta_Y) + \sum_{T}^{E-U} L(Y_T, \hat{Y}_T)$$
(33)

Where, a regularization term r is representing. Both the loss function L and r are assumed possess second derivatives that exist and are continuous with respect to their arguments.

4. Result and Discussion

This section explains the results from the simulation and talks about how well the new method works [25]. The main goal of this method is to use as much renewable energy sources as possible while lowering costs and reducing pollution. The simulation of the CapSA-GR-RNN technique is explained below. The control setup was created in the MATLAB platform, and its performance was compared with other existing methods like PSO, SSA, and GWO. The results are divided into three cases: 1) How well the method works with PV, WT, FC, and a battery. 2) How well the method works with PV, FC, and a battery.

Case 1: Performance analysis of proposed method under PV, WT, FC, Battery

Analysis the power of renewable energy sources (a) generation power 1 (b) generation power 2 is shown in Fig 3. In generation power1, the demand is initially starts from 3kW at 1hour and increases and decreases. Then the demand is finally reach as 2.7kW at 24hour. The PV is initially starts from 1kW at 1hour and increases and decreases. Then the PV is finally reached as 0.9kW at 24hour. The WT is initially starts from 1kW at 1hour and increases and decreases. Then the wind turbine is finally reaches 0.9kW at 24hour. The FC is initially starts from 0kW at 1 hour and increases and decreases. The FC is increase at point 3kW at 2.5hour. Then the FC is finally reaches 0kW at 24hour. The battery is initially starts from 2.3kW at 1hour and increases and decreases. Then the battery is finally reaches 1.7kW at 24hour. These are shown in Fig 3(a). In generation power2, the demand is initially starts from 5.2kW at 1hour and increases and decreases. Then the demand is finally reach as 5.4kW at 24hour. The PV is initially starts from 0kW at 1hour and increases and decreases. Then the PV is finally reached as 0kW at 24hour. The WT is initially starts from 1kW at 1hour and increases and decreases. Then the wind turbine is finally reaches 0.9kW at 24hour. The FC is initially starts from 2kW at 1hour and increases and decreases. Then the FC is finally attains 1kW at 24hour. The battery is initially starts from 0kW at 1hour and increases and decreases. Then the battery is finally attains 0kW at 24hour. These are shown in Fig 3(b).



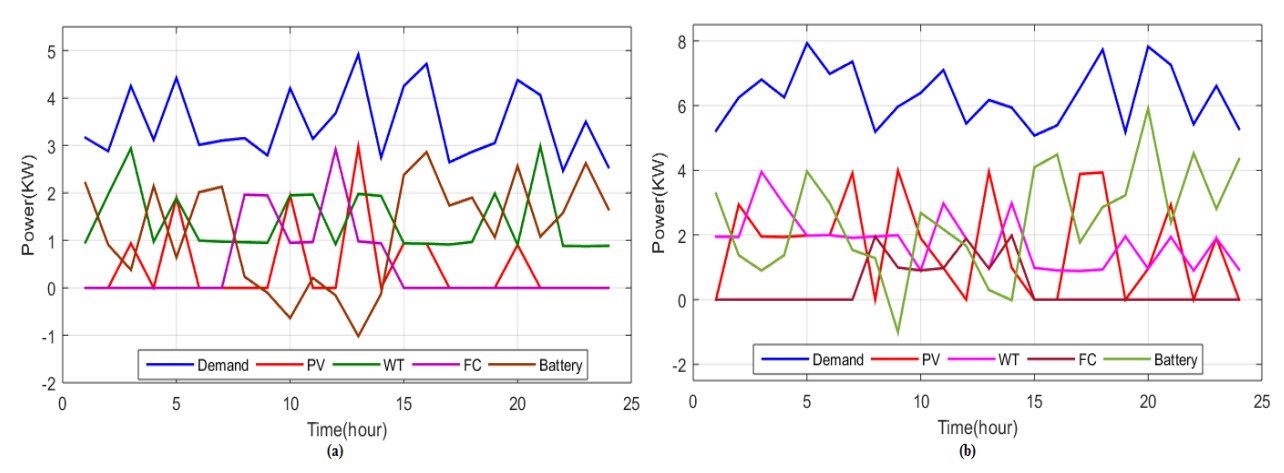


Fig 3: Analysis the power of renewable energy sources (a) generation power 1 (b) generation power 2.

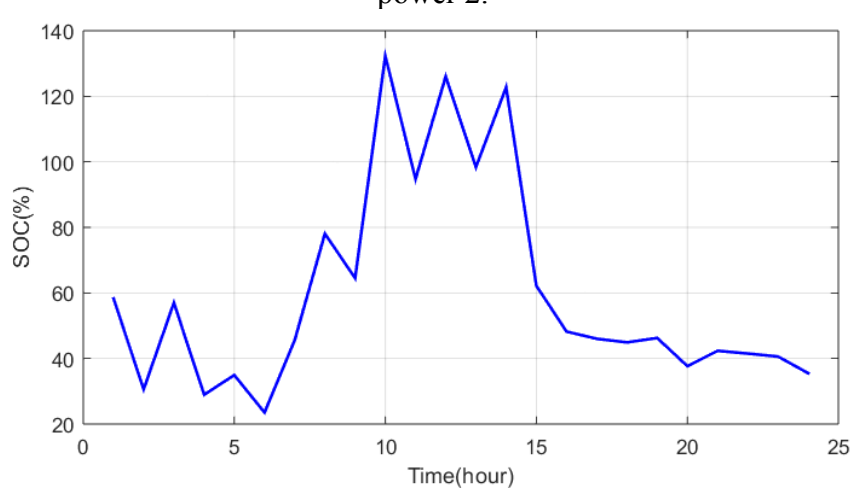


Fig 4: Analysis the SOC



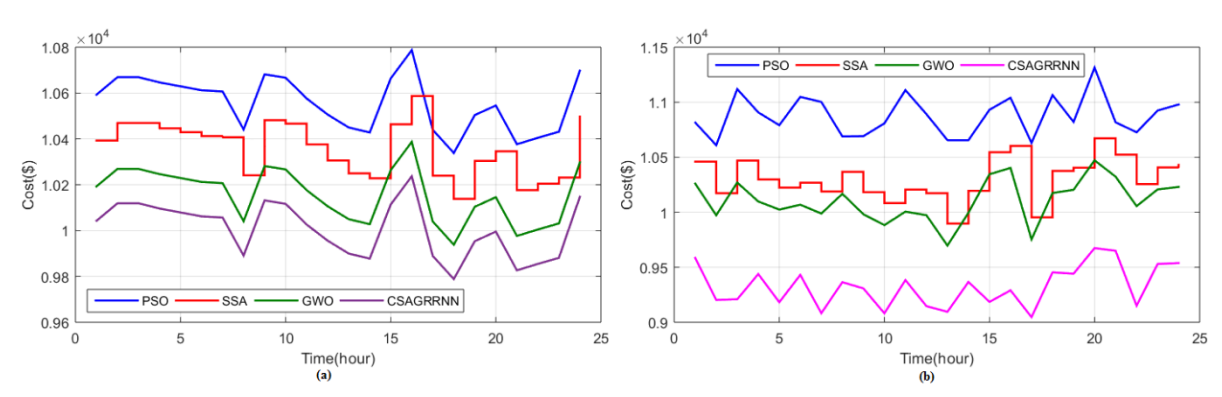


Fig 5: Comparison of cost for existing and proposed approach (a) Jan cost (b) July cost Analysis the SOC is shown in Fig 4. The SoC is initially starts from 60% at 3hour and increase and decreases. The SoC is increase at point 135% at 10hour and then finally reach as 38 % at 24hour. Comparison of cost for existing and proposed approach (a) Jan cost (b) July cost is shown in Fig 5. In PSO approach the cost is 1.08\$ In SSA approach the cost is 1.06\$. In GWO approach the cost is 1.04\$. In proposed approach the cost is 1.2\$In SSA approach the cost is 1.06\$. In GWO approach the cost is 1.04\$. In proposed approach the cost is 0.97\$ which is lower than other existing system. These are displayed in Fig 5(b).

Case 2: Performance analysis of proposed method under PV, FC, Battery

Analysis the power depicted in Figure 6 illustrates the dynamics of various energy sources and their contributions over a 24hour. Initially, in the generation power1, the demand commences at 5 kW at 1 hour and fluctuates over time, eventually stabilizing at 5.2 kW by the 24th hour. Concurrently, the PV generation initiates at 0.9 kW at 1 hour, exhibiting fluctuations throughout the day, and culminates at 3 kW by the 24th hour. The FC contribution begins at 0 kW at 1 hour and fluctuates until a notable increase to 5 kW is observed at the 13th hour, before tapering off to 0 kW by the 24th hour. Regarding the battery, its discharge initiates at 4.2 kW at 1 hour, experiencing fluctuations similar to the other sources, and ultimately decreases to 2.3 kW by the 24th hour.

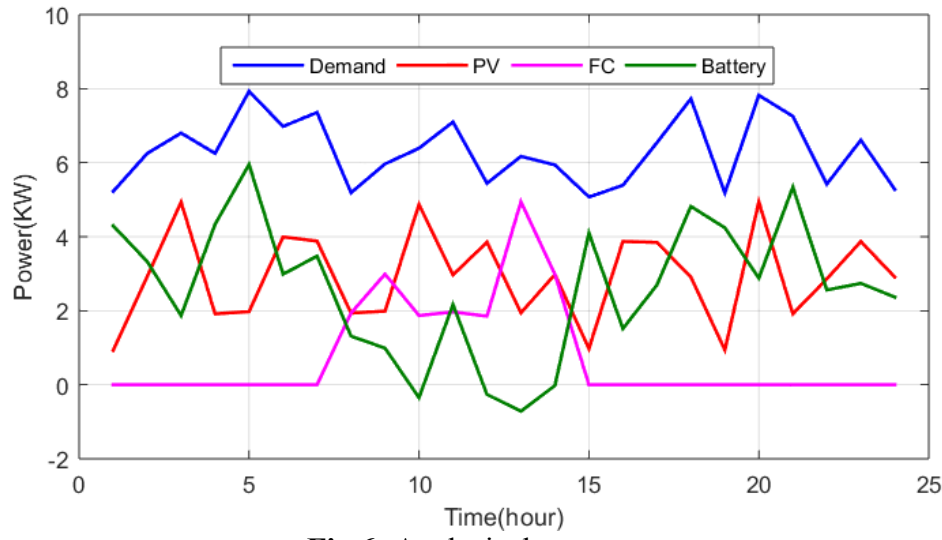


Fig 6: Analysis the power



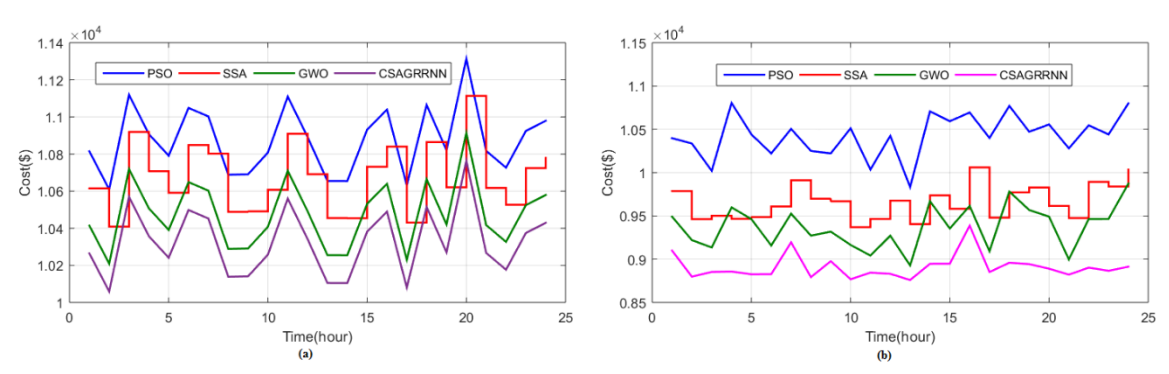


Fig 7: Cost comparison between the proposed and existing approaches (a) Jan cost (b) July cost Cost comparison between the proposed approach and existing methods is shown in Figure 7. For January, the PSO method costs \$1.10, SSA costs \$1.09, GWO costs \$1.07, and the proposed method costs \$1.05, which is the lowest. These results are shown in Figure 7(a). For July, the PSO method costs \$1.08, SSA costs \$0.98, GWO costs \$0.96, and the proposed method costs \$0.93, which is again the lowest. These results are shown in Figure 7(b).

Case 3: Performance analysis of proposed method under WT, FC, Battery

Analysis the power of renewable energy sources (a) generation power 1 (b) generation power 2 is shown in Fig 9. In generation power1, the demand initially starts at 3.2 kW at 1 hour and fluctuates throughout the 24hour, ultimately reaching 2.7 kW. The WT begins at 3 kW at 1 hour, fluctuates, and eventually diminishes to 0 kW by the 24th hour. The FC starts at 1 kW at 1 hour, experiences fluctuations, and notably increases to 4 kW at the 12.5th hour before returning to 0 kW by the end of the 24hour. The battery starts at -1.03 kW at 1 hour, fluctuates, and finally reaches 1.8 kW by the 24th hour. These data are depicted in Fig 9(a). In generation power2, the demand starts at 5.4 kW at 1 hour and fluctuates similarly to power1, reaching 5.5 kW by the 24th hour. The WT, beginning at 3 kW at 1 hour, also experiences fluctuations and diminishes to 0 kW by the end of the 24-hour. The FC begins at 1 kW at 1 hour, fluctuates, and eventually decreases to 0.9 kW by the 24th hour. The battery, starting at -1.1 kW at 1 hour, fluctuates and finally reaches 2 kW by the 24th hour. These details are illustrated in Fig 9(b).

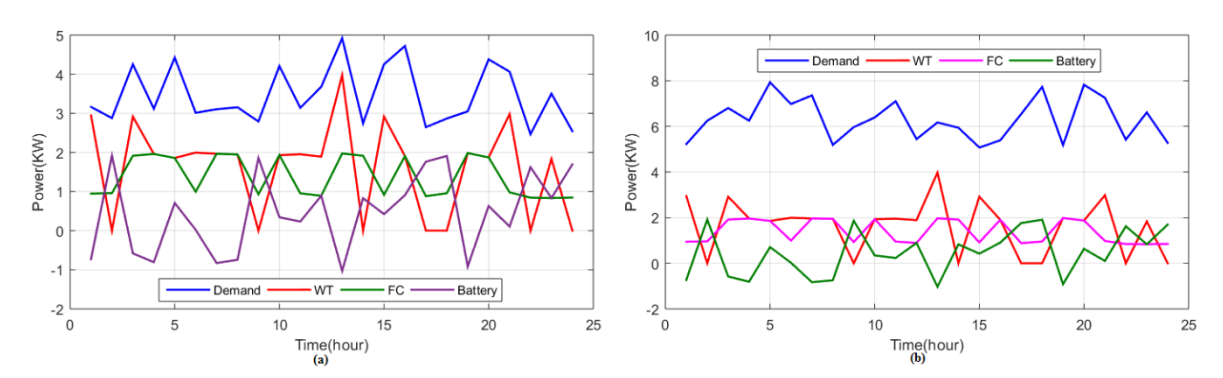


Fig 9: Analysis the power of renewable energy sources (a) generation power 1 (b) generation power 2



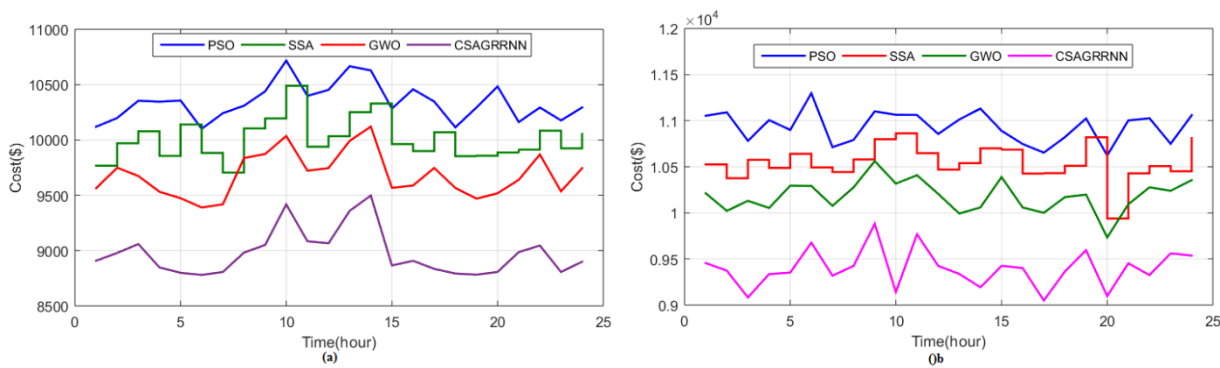


Fig 10: Cost comparison between the proposed and existing approaches (a) Jan cost (b) July cost The comparison of costs between the new method and the current methods is shown in Figure 10. For January costs, the PSO method costs \$10,700, the SSA method costs \$10,500, the GWO method costs \$10,000, and the new method costs \$9,500, which is less than the other methods. These results are shown in Figure 10(a). For July costs, the PSO method costs \$1.13, the SSA method costs \$1.08, the GWO method costs \$1.05, and the new method costs \$0.98, which is again lower than the other methods. These results are shown in Figure 10(b).4.1. Discussion The analysis conducted across three cases offers valuable insights into the performance and cost efficiency of renewable energy systems, comparing existing methodologies with the proposed approach. In Case 1, the examination of power generation and state of charge reveals the intricate interplay among demand, renewable energy sources, and storage technologies. Notably, the proposed method consistently showcases lower costs than current approaches, demonstrating its effectiveness in both January and July scenarios. Case 2 further underscores the efficacy of the proposed approach in optimizing power generation and reducing expenses. Despite fluctuations in demand and renewable energy output, the proposed method consistently outperforms existing strategies, delivering significant cost savings. Lastly, in Case 3, a thorough analysis of power generation across different scenarios highlights the versatility of the proposed approach in managing varying demand and renewable energy availability. The cost comparison underscores the superior cost-effectiveness of the proposed method across diverse scenarios and seasonal variations. Overall, these results indicate that the proposed approach not only efficiently handles power generation and storage but also offers substantial cost reductions compared to existing methods across various scenarios and timeframes. These findings suggest promising prospects for widespread adoption of the proposed approach, attractive both sustainability and economic viability in renewable energy systems.

5. Conclusion

This study introduces a combined method for a smart grid system that uses a lot of renewable energy sources. Since one algorithm might not work well in all situations, the study uses two algorithms together: CapSA and GR-RNN. The GR-RNN part helps predict how renewable sources like solar and wind will behave, such as their probability and distribution. The CapSA part helps make the smart microgrids work as well as possible. The main aim of this method is to make the most use of renewable energy while keeping costs low and reducing pollution. The method was tested using MATLAB and compared with other commonly used methods. The results show that the proposed method works superior than methods like PSO, SSA, and GWO. The cost was found to be \$1.08 with PSO, \$0.93 with the proposed method, \$0.98 with SSA, and \$0.96 with GWO. Future research should focus on improving and expanding this hybrid



approach for smart grids with a lot of renewable energy. This could include using more optimization techniques and machine learning to make the system more accurate and efficient. Looking into new algorithms or mixing existing ones might provide new ideas for managing smart grids with different renewable sources. Also, using real-time data and better predictive models could help make smarter decisions in the grid. Studying the economic impact and how well this method can be scaled up will help understand if it's practical and sustainable in the long run. Checking how technologies like blockchain or IoT can be used to manage data and security in smart grids could lead to more progress in this area.

Reference

- [1] Liang, K., Wang, H., Pozo, D., & Terzija, V. (2024). Power system restoration with large renewable penetration: State-of-the-art and future trends. International Journal of Electrical Power & Energy Systems, 155, 109494.
- [2] Liu, S., Yan, J., Yan, Y., Zhang, H., Zhang, J., Liu, Y., & Han, S. (2024). Joint operation of mobile battery, power system, and transportation system for improving the renewable energy penetration rate. Applied Energy, 357, 122455.
- [3] Fotopoulou, M., Rakopoulos, D., Petridis, S., & Drosatos, P. (2024). Assessment of smart grid operation under emergency situations. Energy, 287, 129661.
- [4] Al Talaq, M., & Al-Muhaini, M. (2024). Optimal coordination of time delay overcurrent relays for power systems with integrated renewable energy sources. In Power System Protection in Future Smart Grids (pp. 81-107). Academic Press.
- [5] Aygul, K., Mohammadpourfard, M., Kesici, M., Kucuktezcan, F., & Genc, I. (2024). Benchmark of machine learning algorithms on transient stability prediction in renewable rich power grids under cyberattacks. Internet of Things, 25, 101012.
- [6] Saha, S., Saleem, M. I., & Roy, T. K. (2023). Impact of high penetration of renewable energy sources on grid frequency behaviour. International Journal of Electrical Power & Energy Systems, 145, 108701.
- [7] Ghirardi, E., Brumana, G., Franchini, G., & Perdichizzi, A. (2023). H2 contribution to power grid stability in high renewable penetration scenarios. International Journal of Hydrogen Energy, 48(32), 11956-11969.
- [8] Ghirardi, E., Brumana, G., Franchini, G., & Perdichizzi, A. (2023). H2 contribution to power grid stability in high renewable penetration scenarios. International Journal of Hydrogen Energy, 48(32), 11956-11969.
- [9] Zhao, N., Zhang, H., Yang, X., Yan, J., & You, F. (2023). Emerging information and communication technologies for smart energy systems and renewable transition. Advances in Applied Energy, 100125.
- [10] Jirdehi, M. A., & Tabar, V. S. (2023). Risk-aware energy management of a microgrid integrated with battery charging and swapping stations in the presence of renewable resources high penetration, crypto-currency miners and responsive loads. Energy, 263, 125719.
- [11] Secchi, M., Barchi, G., Macii, D., & Petri, D. (2023). Smart electric vehicles charging with centralised vehicle-to-grid capability for net-load variance minimisation under increasing EV and PV penetration levels. Sustainable Energy, Grids and Networks, 35, 101120.
- [12] Fotopoulou, M., Rakopoulos, D., Petridis, S., & Drosatos, P. (2024). Assessment of smart grid operation under emergency situations. Energy, 287, 129661.
- [13] Akhtar, I., Kirmani, S., & Jameel, M. (2021). Reliability assessment of power system considering the impact of renewable energy sources integration into grid with advanced intelligent strategies. IEEE Access, 9, 32485-32497.
- [14] Liang, K., Wang, H., Pozo, D., & Terzija, V. (2024). Power system restoration with large renewable penetration: State-of-the-art and future trends. International Journal of Electrical Power & Energy Systems, 155, 109494.



- [15] Saha, S., Saleem, M. I., & Roy, T. K. (2023). Impact of high penetration of renewable energy sources on grid frequency behaviour. International Journal of Electrical Power & Energy Systems, 145, 108701.
- [16] Wang, S., Li, F., Zhang, G., & Yin, C. (2023). Analysis of energy storage demand for peak shaving and frequency regulation of power systems with high penetration of renewable energy. Energy, 267, 126586.
- [17] Wang, L., Jiang, S., Shi, Y., Du, X., Xiao, Y., Ma, Y., ... & Li, M. (2023). Blockchain-based dynamic energy management mode for distributed energy system with high penetration of renewable energy. International Journal of Electrical Power & Energy Systems, 148, 108933.
- [18] Hashimoto, J., Ustun, T. S., Suzuki, M., Sugahara, S., Hasegawa, M., & Otani, K. (2021). Advanced grid integration test platform for increased distributed renewable energy penetration in smart grids. Ieee Access, 9, 34040-34053.
- [19]Kannan, E., Avudaiappan, M., Kaliyaperumal, S., Muthusamy, S., Pandiyan, S., Panchal, H., ... & Shanmugam, C. (2023). A novel single phase grid connected solar photovoltaic system for state of charge estimation using recurrent neural networks. *Energy Sources, Part A: Recovery, Utilization, and Environmental Effects*, 45(1), 841-859.
- [20] Singh, S., Chauhan, P., & Singh, N. J. (2020). Feasibility of grid-connected solar-wind hybrid system with electric vehicle charging station. *Journal of Modern Power Systems and Clean Energy*, 9(2), 295-306.
- [21] Belkhier, Youcef, Adel Oubelaid, and Rabindra Nath Shaw. "Hybrid power management and control of fuel cells battery energy storage system in hybrid electric vehicle under three different modes." *Energy Storage* 6.1 (2024): e511.
- [22] Jia, Jiandong, et al. "Multi-objective optimization study of regional integrated energy systems coupled with renewable energy, energy storage, and inter-station energy sharing." *Renewable Energy* 225 (2024): 120328.
- [23] Braik, Malik, Alaa Sheta, and Heba Al-Hiary. "A novel meta-heuristic search algorithm for solving optimization problems: capuchin search algorithm." *Neural computing and applications* 33 (2021): 2515-2547.
- [24] He, Sheng, and Lambert Schomaker. "GR-RNN: Global-context residual recurrent neural networks for writer identification." *Pattern Recognition* 117 (2021): 107975.
- [25] Guangqian, Du, et al. "A hybrid algorithm based optimization on modeling of grid independent biodiesel-based hybrid solar/wind systems." *Renewable Energy* 122 (2018): 551-560.